

Composition of Safety Constraints For Fixed-Wing Collision Avoidance Amidst Limited Communications

Eric Squires* and Pietro Pierpaoli†
Georgia Institute of Technology, Atlanta, GA 30318

Rohit Konda‡
University of California Santa Barbara, Santa Barbara, California 93106

Samuel Coogan§ and Magnus Egerstedt¶
Georgia Institute of Technology, Atlanta, GA 30318

This paper considers how to ensure that a system of fixed wing Unmanned Aerial Vehicles (UAVs) can avoid collisions. To do so we develop a novel method for creating a barrier function, which is similar to a Lyapunov function and can be used to ensure that a system can stay safe for all future times. After introducing the general approach, it is shown how to ensure that collision avoidance for two vehicles can be guaranteed for all future times. The construction is then extended to the case of arbitrarily many vehicles by addressing how to satisfy multiple safety objectives simultaneously. We do this while ensuring output actuator commands are within specified limits. Because this formulation requires communication of control values and may therefore reduce throughput of other important messages, we then show how to reformulate the solution without this significant communication overhead while still ensuring safety is maintained and actuator limits are respected. We validate the theoretical developments of this paper in the simulator SCRIMMAGE with a simulation of 20 UAVs that maintain safe distances from each other even though their nominal paths would otherwise cause a collision.

I. Introduction

As low-cost, unmanned aerial vehicles (UAVs) find civilian uses, the low-altitude airspace is increasingly congested, leading to large-scale UAV operation limitations including concerns for privacy, the environment, national security, and safe-flight validation [1]. A key challenge for safe-flight validation in congested environments is ensuring collision avoidance while enabling vehicles to accomplish their designed missions. Thus, in this paper we propose an algorithm that minimally alters a vehicle's nominal control input while still ensuring safe operations.

*Research Engineer, Aerospace, Transportation and Advanced Systems Laboratory of the Georgia Tech Research Institute; eric.squires@gtri.gatech.edu.

†Postdoc, Electrical and Computer Engineering; pietro.pierpaoli@gatech.edu.

‡PhD student, Electrical and Computer Engineering.

§Assistant Professor, School of Electrical and Computer Engineering as well as the School of Civil and Environmental Engineering; sam.coogan@gatech.edu.

¶Chair, School of Electrical and Computer Engineering; magnus.egerstedt@ece.gatech.edu.

A variety of approaches to fixed-wing collision avoidance have been proposed. Partially observable Markov decision processes are used in [2, 3] to achieve safe flight distances. The dynamic window approach, originally introduced in [4] for static obstacles and adapted to moving obstacles in [5], uses circular arcs for trajectories and limits the set of allowable velocities to enable a quick optimization of the control input. In [6], the authors develop a first-order look-ahead algorithm that can be applied to vehicles with unicycle dynamics in a decentralized way while guaranteeing that collisions amongst k vehicles are avoided. Potential functions [7, 8] have also been applied to fixed-wing collision avoidance, where it can be shown that vehicles can safely avoid each other even when their sensing range is limited. Similarly, [9] discusses how to combine potential functions with trajectory goals into a navigation function in order to provide criteria under which collision avoidance can be guaranteed. Navigation functions have also been combined with Model Predictive Control (MPC) by making inter-agent distance requirements implicit in the cost function [10]. MPC has additionally been applied to UAV collision avoidance for vehicles with limited sensing [11] and communication constraints [12]. While MPC provides a flexible framework for distributed collision avoidance, its limited horizon can make safety guarantees difficult. In a more general case, the optimal control formulation in [13] allows for collision avoidance guarantees, but it is computationally intensive as it requires numerically solving the Hamilton-Jacobi-Bellman equations over an infinite horizon.

Trajectory generation was analyzed in [14] where a nonlinear program is developed to find a safe reference trajectory constructed from polynomials. In [15] and [16], the authors discuss trajectory generation using a RRT with dynamics constraints provided by dubins paths and a waypoint generation algorithm, respectively. Finally, in [17], the authors also consider a trajectory based approach to avoid static obstacles. Similar to evasive maneuvers, traffic rules [18, 19] are a method for encoding hybrid behaviors that can include collision avoidance trajectories. In [18], the authors show that a two vehicle system with limited sensing range can avoid collisions while reaching position goals. While in general this may result in conservative behaviors, they demonstrate in simulation that the decentralized algorithm continues to allow vehicles to reach their target configuration while avoiding collisions for as many as 70 vehicles. Reactive methods are useful because they can often be calculated online while evasive maneuvers benefit from a lookahead into the future. In this paper we leverage the merits of both approaches within the framework of control barrier functions.

Motivated by the importance of formal guarantees of collision avoidance that are computationally feasible and minimally invasive we discuss in this paper how to apply barrier functions (e.g., [20], [21]) to the UAV collision avoidance problem, where the system is subject to actuator constraints, nonlinear dynamics, and nonlinear safety constraints. Barrier functions are similar to Lyapunov functions and allow for guarantees that a system will stay safe (i.e., vehicles will maintain safe distances from each other) for all future times. Further, under some assumptions detailed in Section II, a Quadratic Program (QP) can be used to calculate a safe control input implied by a barrier function so that the calculation can be done online [21]. Given such safety guarantees, barrier functions have been applied to a set of problems including collision avoidance for autonomous agents ([22, 23]), bipedal robots ([24, 25]), adaptive cruise

control and lane following ([21, 26–28]), and in mobile communication networks [29].

However, barrier functions rely on being able to find a function for safety set invariance to be guaranteed. For systems like a fixed wing UAV with actuator constraints, nonlinear dynamics, and nonlinear safety constraints, generating such a function can be difficult. In this respect they are similar to Lyapunov functions. They provide guarantees when a system designer can find appropriate functions but they may be difficult to construct.

Nevertheless, there are a variety of approaches to finding a barrier function given a system and safety constraints. One approach discussed for instance in ([20, 26, 30, 31]), uses a sum of squares decomposition [32]. In this approach an initially conservative estimate for a barrier function is found and the associated safe set is iteratively enlarged. Iterative approaches have also been developed when the system has relative degree greater than one. The conditions for calculating a safe control input for higher order systems are given in [33]. In [25], a backstepping approach is developed that ensures a control barrier function can be constructed and a similar approach is discussed in [34]. The approach discussed in this paper is most similar to [35] where a barrier function is formulated by calculating the distance to a backup set after applying a backup controller. In this paper we develop an alternative approach that does not require the specification of a backup set.

System-specific arguments have also been applied to the development of a barrier function. For instance, geometric insights are exploited in [24], where the authors develop a barrier function for precise foot placement by ensuring that the foot is within the intersection of two circles. Similarly, in [22, 23], the authors develop a barrier function that ensures a circle and ellipsoid, respectively, around each robot will not overlap in order to ensure there will be no collisions for double integrator and quadrotor robots, respectively. Barrier functions have also been developed for unicycle dynamics in [28], where the dynamics are simplified by considering a point slightly in front of the vehicle.

Previous work on barrier functions has shown how, given the current state, a safe control input can be selected to ensure the system is safe for all times. In this paper, we also ensure system safety but do so by integrating the dynamics into the future using a known evasive maneuver that is always available to keep the system safe. In this respect the system is more predictable since it is known that a particular control input will be safe. Further, we ensure that actuator limits are respected which is a significant constraint in the case of UAVs where the system has non-zero minimum velocity.

Aside from ensuring a barrier function constraint can be satisfied given actuator limitations, UAV collision avoidance also motivates the consideration of multiple safety constraints that must be satisfied at all times. In particular, because collision avoidance can be viewed as a constraint for each pairwise combination of vehicles [29, 36], we briefly review how barrier functions have been applied to systems with multiple constraints. A contract-based approach is presented in [26]. A sum of squares decomposition is presented in [31] where additional safety constraints map to additional constraints in the optimization problem. In [34], necessary and sufficient conditions are given for the existence of a control input that satisfies multiple barrier function constraints. The approach generalizes to high order and time-varying

systems but requires that actuator constraints be unbounded. Barrier function composition has also been addressed in [26, 29, 36]. In [26], the authors partition the state space into regions for which a single barrier function is active in each component of the partition. In [29] and [36] non-smooth barrier functions are discussed, where the result allows for combining barrier functions using boolean primitives. One drawback of the boolean composition approaches is that it is not guaranteed that the composition of barrier functions will result in a barrier function.

The high level contribution of the paper is a method for constructing a barrier function given a safety constraint and system dynamics. In particular, after a safety engineer specifies an evasive maneuver we then show how to construct a barrier function. This paper makes the following technical contributions. First, it generalizes a method discussed in [22, 23] for constructing a barrier function that can be used to make safety guarantees for a system. Second, it examines how to ensure that multiple safety constraints can be satisfied simultaneously when using this constructive method. Third, it presents an algorithm for ensuring safety in the context of multi-agent systems that does not require communication of low level actuator commands. Fourth, it shows how to apply the above theory to a scenario involving fixed wing UAVs where vehicles must ensure minimum separation distances are maintained at all times. This paper expands on the conference version [37] which did not consider multiple constraints and did not consider limited communications. Finally, this paper expands on the simulation study presented in [37] by considering a scenario with 20 vehicles to demonstrate that all pairwise distances between vehicles can be kept above a minimum safety distance throughout a scenario.

This paper is organized as follows. Section II discusses background information for barrier functions. Section III discusses a general method for constructing a barrier function and shows how to apply it to fixed wing collision avoidance. Section IV generalizes the results of Section III by showing how to satisfy multiple constraints simultaneously. Section V relaxes the amount of information required to share between vehicles while still guaranteeing safety. Section VI presents a simulation verification of the approach. Section VII concludes.

II. BARRIER FUNCTIONS BACKGROUND

We summarize the necessary background for barrier functions here. See [21] for further discussion. Consider a control affine system

$$\dot{x} = f(x) + g(x)u \quad (1)$$

where f and g are locally Lipschitz functions, $x \in \mathbb{R}^n$, $u \in U \subset \mathbb{R}^m$, and solutions are forward complete, meaning the system has a unique solution for all time $t \geq 0$ given a starting condition $x(0)$.

We expand this formulation to a set of k vehicles by considering each vehicle's state x_i and dynamics $\dot{x}_i = f_i(x_i) + g_i(x_i)u_i$ where $x_i \in \mathbb{R}^{n_i}$, $u_i \in U_i \subseteq \mathbb{R}^{m_i}$ and $i \in \{1, \dots, k\}$. The overall state for the system is described by $x = \begin{bmatrix} x_1^T & x_2^T & \dots & x_k^T \end{bmatrix}^T \in \mathbb{R}^n$ where $n = \sum_{i=1}^k n_i$ and $u = \begin{bmatrix} u_1^T & u_2^T & \dots & u_k^T \end{bmatrix}^T \in U_1 \times U_2 \times \dots \times U_k = U \subset \mathbb{R}^m$,

where $m = m_1 + \dots + m_k$. In this case, (1) can be represented as

$$\dot{x} = \begin{bmatrix} f_1(x_1) \\ f_2(x_2) \\ \vdots \\ f_k(x_k) \end{bmatrix} + \begin{bmatrix} g_1(x_1) & 0 & \dots & 0 \\ 0 & g_2(x_2) & \dots & 0 \\ \vdots & \vdots & \ddots & \vdots \\ 0 & 0 & \dots & g_k(x_k) \end{bmatrix} \begin{bmatrix} u_1 \\ u_2 \\ \vdots \\ u_k \end{bmatrix}.$$

Considering small bank and pitch angles, the state and control input to the single vehicle are described by $x_i = \begin{bmatrix} p_{i,x} & p_{i,y} & \theta_i & p_{i,z} \end{bmatrix}^T$ and $u_i = \begin{bmatrix} v_i & \omega_i & \zeta_i \end{bmatrix}^T$ respectively, while lateral and vertical kinematics can be described as [6, 8–10, 18, 19]:

$$\dot{x}_i = \begin{bmatrix} \cos(\theta_i) & 0 & 0 \\ \sin(\theta_i) & 0 & 0 \\ 0 & 1 & 0 \\ 0 & 0 & 1 \end{bmatrix} \begin{bmatrix} v_i \\ \omega_i \\ \zeta_i \end{bmatrix}, \quad (2)$$

where the sets of bounded control inputs are $v_i \in [v_{min}, v_{max}]$ with $v_{min} > 0$, $|\omega_i| \leq \omega_{max}$, $|\zeta_i| \leq \zeta_{max}$.

Suppose the set of desired configurations is described by the superlevel set of an output function $h : \mathbb{R}^n \rightarrow \mathbb{R}$ defined on an open set $\mathcal{D} \subseteq \mathbb{R}^n$. The superlevel set of h is then called the safe set and is defined as

$$C = \{x \in \mathcal{D} : h(x) \geq 0\}. \quad (3)$$

The objective is now to establish the condition under which the state system belongs to C for all times.

Definition 1. [21] Given a set $C \subset \mathbb{R}^n$ defined in (3) for a continuously differentiable function $h : \mathbb{R}^n \rightarrow \mathbb{R}$, the function h is called a *zeroing control barrier function (ZCBF)* defined on an open set \mathcal{D} with $C \subset \mathcal{D} \subset \mathbb{R}^n$, if there exists a Lipschitz continuous extended class \mathcal{K} function α such that

$$\sup_{u \in U} [L_f h(x) + L_g h(x)u + \alpha(h(x))] \geq 0, \quad \forall x \in \mathcal{D}. \quad (4)$$

In the above definition $L_f h(x) = \frac{\partial h(x)}{\partial x} f(x)$ and $L_g h(x) = \frac{\partial h(x)}{\partial x} g(x)$ denote the Lie derivatives. From Definition 1, it follows that the admissible control space is defined as

$$K(x) = \{u \in U : L_f h(x) + L_g h(x)u + \alpha(h(x)) \geq 0\}. \quad (5)$$

Theorem 1. [21] Given a set $C \subset \mathbb{R}^n$ defined in (3) for a continuously differentiable function h , if h is a ZCBF on \mathcal{D} , then any Lipschitz continuous controller $u : \mathcal{D} \rightarrow U$ such that $u(x) \in K(x)$ will render the set C forward invariant.

In [21] it is also shown how to calculate $u(x) \in K(x)$ using a Quadratic Program (QP) to support fast, online calculations. In particular, assume there is some nominal control input $\hat{u} \in \mathbb{R}^m$ available that is designed to achieve some performance goal (e.g., path-following) that has not necessarily been designed to satisfy safety constraints. Additionally, we assume U can be expressed as the set of all u satisfying the linear inequality $Au \geq b$. A safe control input can then be calculated using the following Quadratic Program (QP)

$$u^* = \min_{u \in \mathbb{R}^m} \frac{1}{2} \|u - \hat{u}\|^2 \quad (6a)$$

$$\text{s.t.} \quad L_f h(x) + L_g h(x)u + \alpha(h(x)) \geq 0 \quad (6b)$$

$$Au \geq b. \quad (6c)$$

Note that by property (4), when h is a ZCBF, (6) is guaranteed to be feasible when $x \in \mathcal{D}$.

III. BARRIER FUNCTION CONSTRUCTION

In general, in order to apply the barrier function framework discussed in the previous section, one needs to define an appropriate barrier function $h(x)$ representative of the collision avoidance constraints the UAVs must satisfy. To this end, as shown in the following example, the design of a suitable barrier function for fixed wing vehicles is not trivial.

A. Motivating Example

In this section we discuss some difficulties with applying barrier functions to the fixed-wing collision avoidance problem via a concrete example. Consider a candidate ZCBF, h , that encodes a collision avoidance safety constraint in a system of two vehicles with state $x = \begin{bmatrix} x_1^T & x_2^T \end{bmatrix}^T$ and

$$h(x) = d_{1,2}(x) - D_s^2, \quad (7)$$

where

$$d_{1,2}(x) = (p_{1,x} - p_{2,x})^2 + (p_{1,y} - p_{2,y})^2 + (p_{1,z} - p_{2,z})^2$$

is the squared distance between vehicles 1 and 2 and D_s is a positive minimum safety distance. To show why h defined in (7) is not a ZCBF, we present an example where, even though the configuration of the aircraft is safe since $x \in C$, $h(x)$ does not satisfy constraint (4). Let $x_1 = \begin{bmatrix} -D_s/2 & 0 & 0 & \epsilon \end{bmatrix}^T$ and $x_2 = \begin{bmatrix} D_s/2 & 0 & \pi & -\epsilon \end{bmatrix}^T$ for some $\epsilon \geq 0$.

First, we note that for $x = \begin{bmatrix} x_1^T & x_2^T \end{bmatrix}^T \in \mathcal{C}$, $h(x) \geq 0$. Further,

$$\begin{aligned} \sup_{u \in U} [L_f h(x) + L_g h(x)u + \alpha(h(x))] &= \sup_{u \in U} [2(p_{1,x} - p_{2,x})(v_1 \cos \theta_1 - v_2 \cos \theta_2) \\ &\quad + 2(p_{1,y} - p_{2,y})(v_1 \sin \theta_1 - v_2 \sin \theta_2) \\ &\quad + 2(p_{1,z} - p_{2,z})(\zeta_1 - \zeta_2)] \\ &= \sup_{u \in U} [-2D_s(v_1 + v_2) + 2\epsilon(\zeta_1 - \zeta_2)] \\ &= -4D_s v_{min} + 2\epsilon \zeta_{max}. \end{aligned}$$

Since $v_{min} > 0$ and $D_s > 0$, if the two vehicles' initial positions satisfy $0 \leq \epsilon < 2D_s v_{min} / \zeta_{max}$ we observe that the quantity above does not satisfy constraint (4), i.e., $\sup_{u \in U} [L_f h(x) + L_g h(x)u + \alpha(h(x))] < 0$. Therefore, we conclude that $h(x)$ defined in (7) is not a ZCBF. The problem with this candidate ZCBF is that it does not account for the fact that by the time the vehicles are close to colliding, it may be too late to avoid each other due to the limited turning radius and positive minimum velocity.

B. Constructing a Barrier Function via Evading Maneuvers

In order to overcome the difficulties demonstrated in the example of Section III.A, we introduce a method to systematically construct a ZCBF from a safety constraint. Let $\rho : \mathcal{D} \rightarrow \mathbb{R}$ be a *safety function* that represents the safety objective we want to satisfy at all times so that $\rho(x) \geq 0$ indicates that the system is safe. In the example from Section III.A for vehicles i and j ,

$$\rho(x) = d_{i,j}(x) - D_s^2. \quad (8)$$

Second, let $\gamma : \mathcal{D} \rightarrow U$ be a *nominal evading maneuver*. Section III.C discusses specific examples of γ for the UAV collision avoidance problem. For now, assuming γ has been selected, let

$$h(x; \rho, \gamma) = \inf_{\tau \in [0, \infty)} \rho(\hat{x}(\tau)), \quad (9)$$

be a candidate ZCBF where \hat{x} and $\dot{\hat{x}}$ are given by

$$\hat{x}(\tau) = x + \int_0^\tau \dot{\hat{x}}(\eta) d\eta, \quad (10)$$

$$\dot{\hat{x}}(\tau) = f(\hat{x}(\tau)) + g(\hat{x}(\tau))\gamma(\hat{x}(\tau)). \quad (11)$$

We assume in this paper that the solution (10) is in \mathcal{D} for all $\tau \geq 0$ so that $\rho(\hat{x}(\tau))$ is well defined. This choice of a candidate ZCBF h is motivated by the fact that in (9), h measures how close the state will get to the boundary of the safe

set assuming γ is used as the control input for all future time.

In Section III.A we saw that we could not use the Euclidean distance for a ZCBF because when a candidate ZCBF h is defined as in (7), $K(x)$ could be empty for some $x \in \mathcal{D}$. In other words, although $x \in \mathcal{D}$ there was no control input available to keep the system safe. With h defined in (9), this problem is alleviated.

Theorem 2. *Given a dynamical system (1) and a set $C \subset \mathcal{D}$ defined in (3) for a continuously differentiable h defined in (9) with a safety function ρ and locally Lipschitz evading maneuver γ , h satisfies (4) for all $x \in C$. If in addition, $L_g h(x)$ is non-zero for all $x \in \partial C$ and γ maps to values in the interior of U , then h is a ZCBF on an open set \mathcal{D} where $C \subset \mathcal{D}$.*

Proof. We start by assuming $x \in C$ and show that h satisfies (4). Because $x \in C$, $h(x) \geq 0$ so $\alpha(h(x)) \geq 0$. Further, note that $L_f h(x) + L_g h(x)\gamma(x)$ is the derivative along the trajectory of \hat{x} . In other words,

$$L_f h(x) + L_g h(x)\gamma(x) = \lim_{a \rightarrow 0^+} \frac{1}{a} \left(\inf_{\tau \in [a, \infty)} \rho(\hat{x}(\tau)) - \inf_{\tau \in [0, \infty)} \rho(\hat{x}(\tau)) \right). \quad (12)$$

Consider the term inside the parenthesis in (12), namely

$$\inf_{\tau \in [a, \infty)} \rho(\hat{x}(\tau)) - \inf_{\tau \in [0, \infty)} \rho(\hat{x}(\tau))$$

and notice that it is the subtraction of an infimum of the same function ρ evaluated on two different intervals. Further, note that the first interval is a subset of the second interval since a approaches 0 from above. Thus, the term inside the parenthesis on the right hand side of (12) is non-negative so $L_f h(x) + L_g h(x)\gamma(x) \geq 0$. We can then conclude that $L_f h(x) + L_g h(x)\gamma(x) + \alpha(h(x)) \geq 0$ so $\gamma(x) \in K(x)$.

Now assume that $L_g h(x)$ is non-zero for some $x \in \partial C$ and γ maps to values in the interior of U . We will show that there is an open set \mathcal{D} that is a strict superset of C for which (4) holds. Let $x \in \partial C$ be such that $L_g h(x)$ is non-zero and $B(x, \mu)$ be a ball of radius $\mu > 0$ such that for all $z \in B(x, \mu) \setminus C$, $L_g h(z)$ is non-zero. Such a ball exists such that $B(x, \mu) \setminus C$ is nonempty because $L_g h(x)$ is continuous. Let $d(z)$ be a non-zero vector such that $d(z) + \gamma(x) \in U$ where $d(z)$ is a non-zero vector in the direction of $L_g h(z)$. Note that such a vector exists because γ maps to the interior of U . Also note that $L_g h(z)d(z) > 0$. Further restrict μ so that $L_g h(z)d(z) + \alpha(h(z)) \geq 0$ for all $z \in B(x, \mu) \setminus C$. Note that for similar reasons discussed earlier in the proof, $L_f h(z) + L_g h(z)\gamma(z) \geq 0$. Then

$$L_f h(z) + L_g h(z)(\gamma(z) + d(z)) + \alpha(h(z)) \geq L_g h(z)d(z) + \alpha(h(z)) \geq 0.$$

□

Remark 1. The intuitive reason why h is a ZCBF is that whenever $h(x)$ is non-negative, we have by definition a control input γ available to keep the system safe. A geometric view is presented in Figure 1. Note that γ is not the output of the

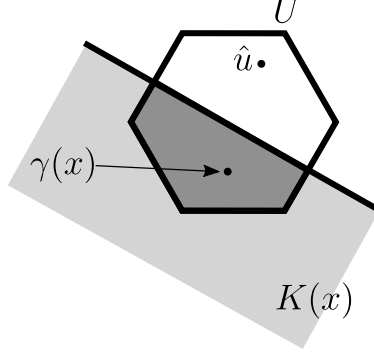


Fig. 1 A geometric view of why h defined in (9) can be a barrier function. Here U is shown as a closed convex polytope satisfying $U = \{u : Au \geq b\}$ and $K(x)$ is the half-space. The constraint (4) implies that the intersection of U and $K(x)$ is non-empty. When h is defined in (9), it satisfies this constraint by ensuring that $\gamma(x) \in U$ and $\gamma(x) \in K(x)$ for all $x \in C$.

Quadratic Program (6). Instead, the role of γ is to allow h to be evaluated via (9).

Remark 2. Theorem 2 holds for any class \mathcal{K} function α . When $\alpha(h(x)) = 0$, (4) becomes $\dot{h}(x) \geq 0$. In other words, Theorem (2) can also be used to prove Lyapunov stability properties of a set by flipping the inequality.

Remark 3. We have found an error in Lemma 1 of the conference version of this paper [37] and Theorem 2 of that paper was based on that Lemma. Therefore Theorem 2 of this paper is reformulated so as not to require that Lemma.

C. Deriving a Barrier Function for UAV Collision Avoidance

We now consider how to calculate h defined in (9) for the UAV collision avoidance problem. From Theorem 2 the only restriction on γ and ρ is that γ is locally Lipschitz and that h is continuously differentiable so there is some flexibility in choosing γ and ρ . In this section we discuss two cases where we can choose γ and ρ so that h can be calculated in closed form. Let the initial state for vehicle i ($i = 1, 2$) be given by $\begin{bmatrix} p_{i,x_0} & p_{i,y_0} & \theta_{i,0} & p_{i,z_0} \end{bmatrix}^T$. For these examples we can calculate h in (9) for arbitrary initial states in closed form. Section IV generalizes the results from Section III.B by showing how to calculate $k(k-1)/2$ barrier functions to ensure that the $k(k-1)/2$ pairwise distance constraints are always satisfied. Because the examples in this section calculate h in (9) using pairwise distance constraints, the calculations in these examples will also apply to the case of more than two vehicles. In other words, with the result of this section we can calculate barrier functions in closed form from arbitrary initial states and numbers of vehicles.

Example 1. In the first case, let

$$\gamma_{turn} = \begin{bmatrix} \sigma v & \omega & 0 & v & \omega & 0 \end{bmatrix}^T \quad (13)$$

with $0 < \sigma \leq 1$, $\omega \neq 0$. In other words, γ_{turn} is defined by the same turn rate for both vehicles but possibly different translational velocities. See Fig. 4a for an example. Define $r = \frac{v}{\omega}$ to be the turn radius of the evasive

maneuver when traveling at speed v , $b_{1,0} = p_{1,x_0} - \sigma r \sin(\theta_{1,0})$, $b_{2,0} = p_{2,x_0} - r \sin(\theta_{2,0})$, $c_{1,0} = p_{1,y_0} + \sigma r \cos(\theta_{1,0})$, $c_{2,0} = p_{2,y_0} + r \cos(\theta_{2,0})$, $\Delta b_0 = b_{1,0} - b_{2,0}$, $\Delta c_0 = c_{1,0} - c_{2,0}$, and $\delta > 0$. Let

$$\rho(x) = d_{1,2}(x) - 2\delta + \delta \sin(\theta_1) - \delta \cos(\theta_1) - D_s^2, \quad (14)$$

where the δ terms are introduced to affect the smoothness of h . See the Appendix for details. Then

$$h(x) = \inf_{\tau \in [0, \infty)} \left(\Delta b_0 + \sigma r \sin(\omega\tau + \theta_{1,0}) - r \sin(\omega\tau + \theta_{2,0}) \right)^2 + \left(\Delta c_0 - \sigma r \cos(\omega\tau + \theta_{1,0}) + r \cos(\omega\tau + \theta_{2,0}) \right)^2 + (p_{1,z_0} - p_{2,z_0})^2 - 2\delta + \delta \sin(\omega\tau + \theta_{1,0}) - \delta \cos(\omega\tau + \theta_{1,0}) - D_s^2.$$

By expanding the square terms and applying two trigonometric identities,* we get

$$h(x) = \inf_{\tau \in [0, \infty)} \Delta b_0^2 + \Delta c_0^2 + (1 + \sigma^2)r^2 - 2\sigma r^2 \cos(\theta_{1,0} - \theta_{2,0}) + 2\sigma \Delta b_0 r \sin(\omega\tau + \theta_{1,0}) - 2\Delta b_0 r \sin(\omega\tau + \theta_{2,0}) - 2\sigma \Delta c_0 r \cos(\omega\tau + \theta_{1,0}) + 2\Delta c_0 r \cos(\omega\tau + \theta_{2,0}) + (p_{1,z_0} - p_{2,z_0})^2 - 2\delta + \delta \sin(\omega\tau + \theta_{1,0}) - \delta \cos(\omega\tau + \theta_{1,0}) - D_s^2. \quad (15)$$

Grouping constant terms and applying phasor addition yields

$$h(x) = \inf_{\tau \in [0, \infty)} A_1 + A_2 \cos(\omega\tau + \Theta) - D_s^2, \quad (16)$$

where A_1 results from grouping constant terms, while A_2 and Θ are the amplitude and phase resulting from the phasor addition so that A_1 and A_2 are functions of x . By convention A_1 and A_2 are nonnegative with appropriate calculation of Θ . The minimum in (16) then occurs at $\tau = (\pi - \Theta + l2\pi)/\omega$ for integers l resulting in nonnegative t so that $h(x) = A_1 - A_2 - D_s^2$. Note that for the case where

$$\rho(x) = \sqrt{d_{1,2}(x) - 2\delta + \delta \sin(\theta_1) - \delta \cos(\theta_1)} - D_s, \quad (17)$$

the same reasoning yields $h(x) = \sqrt{A_1 - A_2} - D_s$ for ρ defined in (17). To ensure that the square root is well defined, we must then require that $A_1 - A_2 \geq 0$ which occurs when the vehicles do not get more than 2δ from each other along the trajectory defined by (10) using γ_{turn} in (13). Since δ can be chosen to be arbitrarily small, it can be chosen so that $\delta \ll D_s$ so the vehicles are very far outside the safe set before this condition occurs.

*The identities are $\sin^2(\alpha) + \cos^2(\alpha) = 1$ and $\cos(\alpha - \beta) = \cos(\alpha)\cos(\beta) + \sin(\alpha)\sin(\beta)$.

Example 2. For a second case, let ρ be given in (8) and

$$\gamma_{straight} = \begin{bmatrix} v_1 & 0 & \zeta_1 & v_2 & 0 & \zeta_2 \end{bmatrix}^T, \quad (18)$$

where $v_1 \neq v_2$. In other words, $\gamma_{straight}$ uses a 0 turn rate while allowing the vehicles to have different speeds. In this case we have

$$h(x) = \inf_{\tau \in [0, \infty)} \left(p_{1,x_0} + \tau v_1 \cos(\theta_{1,0}) - p_{2,x_0} - \tau v_2 \cos(\theta_{2,0}) \right)^2 + \left(p_{1,y_0} + \tau v_1 \sin(\theta_{1,0}) - p_{2,y_0} - \tau v_2 \sin(\theta_{2,0}) \right)^2 + \left(p_{1,z_0} + \tau \zeta_1 - p_{2,z_0} - \tau \zeta_2 \right)^2 - D_s^2, \quad (19)$$

which is quadratic in t so the minimum can be calculated in closed form. See the Appendix for an analysis of the differentiability of h in this case.

The evasive maneuvers in (13) and (18) (when $\zeta_1 = \zeta_2 = 0$ in (18)) both encode trajectories where the vehicles maintain the same altitude for all times and therefore appear to not be exploiting an important evasive capability of the aircraft, namely the ability to change altitudes. However, this is not actually the case. Although γ_{turn} and $\gamma_{straight}$ (for $\zeta_1 = \zeta_2 = 0$) are purely planar maneuvers, they nevertheless can induce behaviors that exploit altitude changes. To see this, note that for h in (16) and (19),

$$\frac{\partial h(x)}{\partial p_{1,z_0}} = 2(p_{1,z_0} - p_{2,z_0}), \quad (20)$$

which is not equal to zero for $p_{1,z_0} \neq p_{2,z_0}$. A similar calculation also holds for $\frac{\partial h(x)}{\partial p_{2,z_0}}$. In other words, h changes as a function of initial altitude. Specifically, this means that the QP can exploit ζ_1 and ζ_2 because the fourth and eighth elements of $L_g h(x(t))$ are non-zero when $p_{1,z_0} \neq p_{2,z_0}$, i.e., the QP in (6) can exploit the altitude control input even though γ_{turn} and $\gamma_{straight}$ do not necessarily include an altitude changing term in the evasive maneuver.

D. Simulation of Two Vehicles

We demonstrate the theoretical development of this section in simulation using SCRIMMAGE [38]. SCRIMMAGE is a multi-agent simulator designed to scale to high numbers of vehicles and includes a plugin-interface that makes it easy to experiment with different motion models and controllers without having to change code. This makes it simple to swap out nominal controllers and vary the fidelity of fixed-wing UAVs from the unicycle dynamics in (2) used in this section up to a 6-DOF model.

For the simulation, let k vehicles be positioned in a circle of radius 200 around the origin, where $k = 2$ in this simulation. In other words, vehicle i has initial state $x_i = \begin{bmatrix} 200 \cos\left(i \frac{2\pi}{k} + \pi\right) & 200 \sin\left(i \frac{2\pi}{k} + \pi\right) & i \frac{2\pi}{k} + \psi & \epsilon_i \end{bmatrix}^T$, where ψ is an additional offset so that vehicles are not necessarily starting with orientation pointing at the origin. The

goal position for vehicle i is on the other side of the origin: $x_{i,g} = \left[200 \cos\left(i\frac{2\pi}{k}\right) \quad 200 \sin\left(i\frac{2\pi}{k}\right) \right]^T$.

This setup is selected so that the vehicles are on a collision course. The nominal controller is that described in [39] with constant $\lambda = 1$. Additionally, we let $v_{min} = 15$ meters/second, $v_{max} = 25$ meters/second, $\zeta_{max} = 3.9$ meters/second, $\omega_{max} = 13$ degrees/second, $D_s = 5$ meters, and $\delta = 0.01$ meters². The choice of ζ_{max} results from assuming a maximum pitch of 15 degrees while traveling at v_{min} . ω_{max} is chosen to be consistent with a constant rate turn [40] with a 30 degree bank with a speed of v_{max} . Each vehicle evaluates (6) at each timestep where we use OSQP [41] to evaluate the QP. We investigate the performance of the vehicles when h defined in (9) is constructed from γ_{turn} in (13) and $\gamma_{straight}$ (18), respectively, where $\gamma_{turn} = \begin{bmatrix} v & \omega & 0 & v & \omega & 0 \end{bmatrix}^T$, $\gamma_{straight} = \begin{bmatrix} v & 0 & 0 & v & 0 & 0 \end{bmatrix}^T$, and $v = 0.9v_{min} + 0.1v_{max}$ and $\omega = 0.9\omega_{max}$. For the scenario with γ_{turn} , we let $\psi = 0$ so that the vehicles start with orientation pointing at the origin. For the scenario with $\gamma_{straight}$, we let $\psi = 2^\circ$ because if the vehicles pointed at the origin they would not start in the safe set. Additionally, for the γ_{turn} case we use ρ in (17). Similarly, for the $\gamma_{straight}$ case we use $\rho(x) = \sqrt{d_{1,2}(x)} - D_s$. Details of the distance between the vehicles and control signals are shown in Figure 2. Note that the resulting trajectory can be different depending on which γ is used as shown in Figure 2d. Nevertheless, in both cases the vehicles are able to maintain safe distances from each other and satisfy actuator constraints throughout the simulation regardless of which γ is used to construct a h .

In the second experiment, we examine the effect of altitude control on the evasive behavior of the aircraft. Because (20) predicts that $\frac{\partial h(x)}{\partial p_{i,z_0}} \neq 0$ (for $i = 1, 2$) only when the vehicles are not at the same altitude, we start the vehicles at an altitude of -1 and 1 , respectively. This offset is small enough to ensure that the nominal path of the vehicles still involves a collision. As was done in the previous experiment, we set $\psi = 0^\circ$ and $\psi = 2^\circ$ degrees when using γ_{turn} and $\gamma_{straight}$, respectively. In Figure 2 we show the output of ζ_1 , where overriding behavior peaks around 8.2 seconds. Notice that the actuator output is within the limits of $\pm\zeta_{max}$. Further, the vehicles maintain safe distances at all times. This occurs even though the evading maneuver does not explicitly encode altitude changes.

IV. COMPOSITION OF MULTIPLE SAFETY CONSTRAINTS

A. Motivating Example

Although the constructive method introduced in (9) can produce a barrier function in the presence of actuator constraints that ensures two vehicles do not collide, the formulation does not extend immediately to collision avoidance for systems with more than two vehicles. To see this, we present a specific example where three UAVs with a collision avoidance safety objective cannot use the results from Section III.B to ensure safety. A plot of this scenario is shown in Figure 4. We index the vehicles by $i = 1, 2, 3$. To ensure collision-free trajectories, and considering the safety function

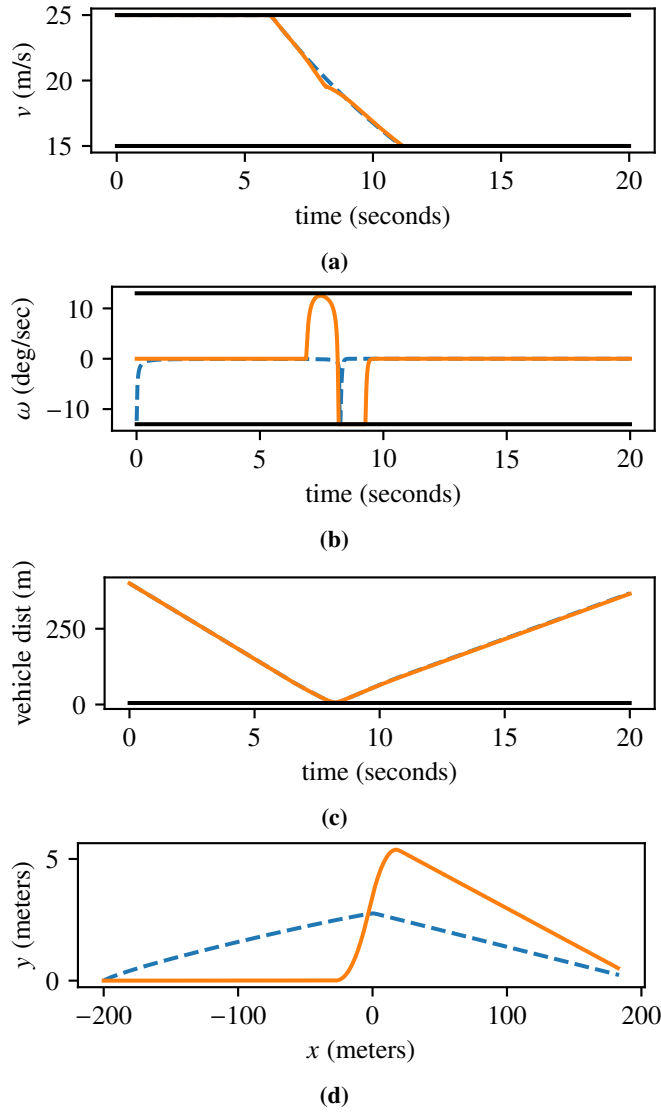


Fig. 2 Outputs for the scenario with 2 fixed-wing vehicles. The blue dashed and orange solid lines are the output of the scenario where h is constructed from $\gamma_{straight}$ and γ_{turn} , respectively. Vehicle 1 velocity and turn rates are shown to be within the actuator limits in (a) and (b). The minimum distance between the vehicles is shown to be above D_s in (c) where the output is very similar in both scenarios. The path taken by vehicle 1 is shown in (d). Note that the choice of γ in constructing h has a significant effect on the path taken.

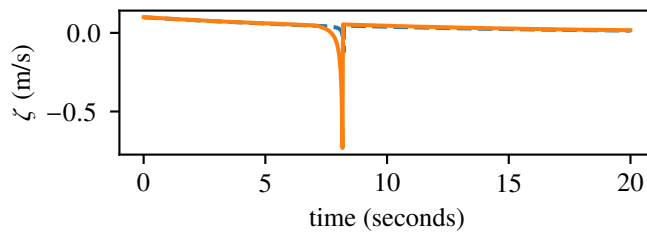


Fig. 3 A plot of ζ_1 as a function of time when h is parameterized by γ_{turn} and $\gamma_{straight}$, respectively. Note the overriding control values around 8.2 seconds and that the values are within $\pm\zeta_{max}$.

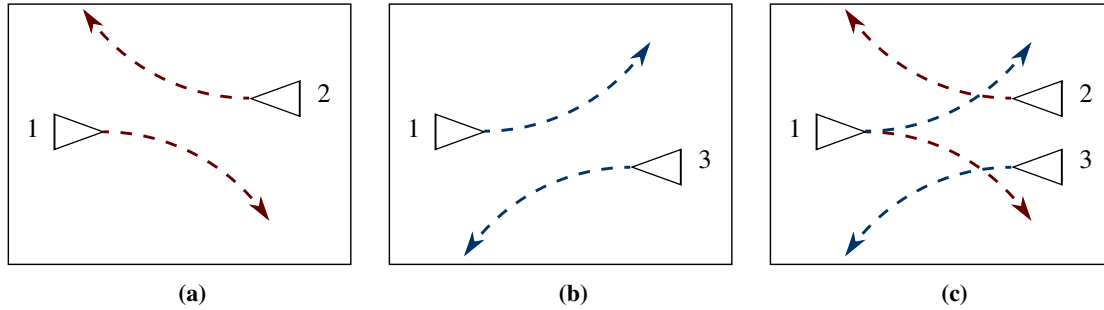


Fig. 4 A geometric view of the example given in Section IV.A. In (a), h^1 defined in (9) is constructed to design a function so that vehicles 1 and 2 stay safe. Here γ^1 encodes an evasive maneuver where vehicles 1 and 2 turn right. Further, vehicles 1 and 2 are placed so that turning right is the only available control input to keep the system safe. In (b), a similar setup is shown for vehicles 1 and 3 where h^2 has been constructed from γ^2 which encodes an evasive maneuver where vehicles 1 and 3 turn left and vehicles 1 and 3 are placed so they are only able to turn left to stay safe. In (c), vehicle 1 cannot turn both right and left to avoid vehicles 2 and 3, respectively. Although vehicle 1 can avoid them individually, it cannot avoid them both simultaneously.

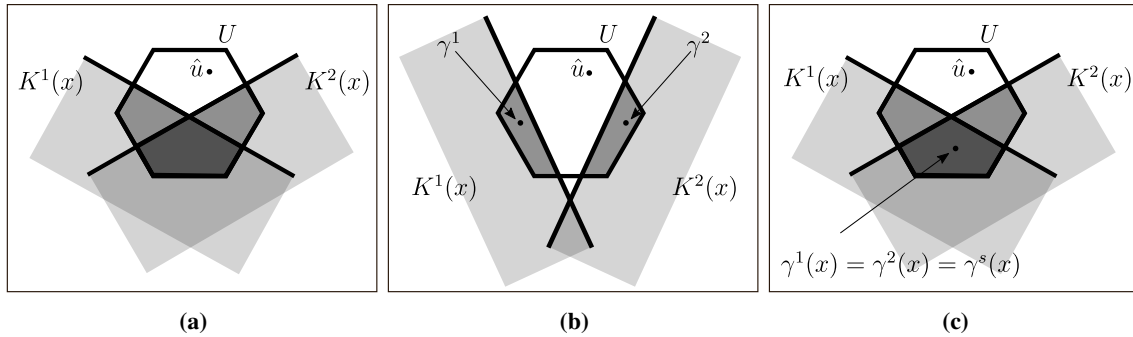


Fig. 5 A geometric view of why having a set of individual barrier functions does not guarantee that a control input u exists to satisfy each associated constraint and how the shared evading maneuver assumption resolves this issue. In (a), multiple barrier function constraints are shown as half-spaces. To satisfy Corollary 1, a u must be selected that is in the intersection of $K^1(x)$, $K^2(x)$, and U . In (b), although there exists a u that is in the intersection of U and $K^1(x)$ as well as U and $K^2(x)$, as guaranteed by the fact that h^1 and h^2 are ZCBFs, there does not exist a u that is in the intersection of U , $K^1(x)$, and $K^2(x)$. This case corresponds to the specific scenario for the three vehicle collision avoidance problem in Fig. 4c. In (c), the problem is resolved by the shared evading maneuver because $\gamma^s(x)$ satisfies each constraint.

defined in (14), three pairwise constraints must be nonnegative at all times:

$$\rho^1(x) = d_{1,2}(x) - 2\delta + \delta \sin(\theta_1) - \delta \cos(\theta_1) - D_s^2,$$

$$\rho^2(x) = d_{1,3}(x) - 2\delta + \delta \sin(\theta_1) - \delta \cos(\theta_1) - D_s^2,$$

$$\rho^3(x) = d_{2,3}(x) - 2\delta + \delta \sin(\theta_2) - \delta \cos(\theta_2) - D_s^2.$$

We now apply the results of Section III to these constraints and for simplicity, let δ be approximately 0. For each constraint, define an arbitrarily chosen nominal evading maneuver

$$\gamma^1(x) = \begin{bmatrix} 1 & -1 & 0 & 1 & -1 & 0 & 1 & -1 & 0 \end{bmatrix}^T \quad (20a)$$

$$\gamma^2(x) = \gamma^3(x) = \begin{bmatrix} 1 & 1 & 0 & 1 & 1 & 0 & 1 & 1 & 0 \end{bmatrix}^T. \quad (20b)$$

In other words, γ^1 encodes an evasive maneuver where all the vehicles turn right while γ^2 and γ^3 encode a maneuver where all the vehicles turn left. We note that h^j ($j = 1, \dots, 3$) defined in (9) and constructed from ρ^j and γ^j are ZCBFs. In this example we let $v_{min} = 1$, $v_{max} = 2$, $\omega_{max} = 1$, and $D_s = 0.5$ so that the vehicles follow a circular trajectory with radius $r = 1$ when applying v_{min} and ω_{max} . Assume now that the vehicles have the following initial states

$$\begin{aligned} x_1 &= \begin{bmatrix} 0 & 0 & 0 & 0 \end{bmatrix}^T, \\ x_2 &= \begin{bmatrix} (2r + D_s) \sin \psi & (2r + D_s) \cos \psi - 2r & \pi & 0 \end{bmatrix}^T, \\ x_3 &= \begin{bmatrix} (2r + D_s) \sin \psi & 2r - (2r + D_s) \cos \psi & \pi & 0 \end{bmatrix}^T, \end{aligned}$$

where $\psi = \arccos\left(\frac{D_s/2+2r}{2r+D_s}\right)$. Then $h^1(x) = h^2(x) = h^3(x) = 0$ and the barrier constraints in (4) for $h^1(x)$ and $h^2(x)$ become

$$-0.4(v_1 + \omega_1 + v_2 + \omega_2) \geq 0 \quad (21)$$

$$0.4(-v_1 + \omega_1 - v_3 + \omega_3) \geq 0. \quad (22)$$

Although h^1 and h^2 are ZCBFs, these two constraints cannot be simultaneously satisfied for $v_i \in [v_{min}, v_{max}]$ and $|\omega_i| \leq \omega_{max}$. In particular, after substituting the minimum velocity $v_1 = v_2 = 1$, the first equation dictates that $\omega_1 + \omega_2 \leq -2$ (i.e., vehicles 1 and 2 must turn right). Similarly, the second equation dictates that vehicle 1 and 3 must turn left. The problem with this scenario is that vehicle 1 cannot simultaneously execute both nominal evading maneuvers (i.e., turn both left and right at the same time). To solve this problem, we will make sure that the evasive

maneuver applied by a vehicle is the same for every barrier function. A geometric view of the general problem and its solution are shown in Figure 5.

B. Sufficient Conditions for Satisfying Multiple Safety Constraints

In order to solve the issues arising when vehicles have to simultaneously respect multiple constraints, we now extend the use of the constructive technique introduced in (9). In this section we extend the reasoning of [21] to the case of q constraints. Consider a nonlinear autonomous system

$$\dot{x} = f(x) \quad (23)$$

where f is locally Lipschitz. Then we have a similar definition to Definition 1 for autonomous systems.

Definition 2. [21] Given a set $C \subset \mathbb{R}^n$ defined in (3) for a continuously differentiable function $h : \mathbb{R}^n \rightarrow \mathbb{R}$, the function h is called a *zeroing barrier function (ZBF)* defined on an open set \mathcal{D} with $C \subset \mathcal{D} \subset \mathbb{R}^n$, if there exists a Lipschitz continuous extended class \mathcal{K} function α such that

$$L_f h(x) \geq -\alpha(h(x)), \forall x \in \mathcal{D}. \quad (24)$$

When there are q constraints, we consider the case of q barrier functions where each barrier function is denoted h^j on \mathcal{D}^j with associated safe set C^j and admissible control space $K^j(x)$ for $x \in \mathcal{D}^j$ for $j \in \{1, \dots, q\}$. We are interested in the conditions under which all safety constraints can be satisfied for all future times. In other words, under the assumption that $x(0) \in C^j$ we want to show that $x(t) \in C^j$ for all $t \geq 0$. Hence, we are interested in the forward invariance of the intersection of all the safe sets, which motivates the following definitions

$$C_\cap = C^1 \cap C^2 \cap \dots \cap C^q, \quad (25)$$

$$K_\cap(x) = \{u \in U : u \in K^1(x) \cap K^2(x) \cap \dots \cap K^q(x)\}. \quad (26)$$

where \mathcal{D}_\cap is an open superset of C_\cap and $x \in \mathcal{D}_\cap$. We can now present a multiple constraint analogue of Theorem 1 by following the same reasoning as [21].

Proposition 1. *Given a dynamical system (23) and a set C_\cap defined by (25) for continuously differentiable functions $h^j : \mathbb{R}^n \rightarrow \mathbb{R}$ where h^j is a ZBF on \mathcal{D}^j with $C^j \subset \mathcal{D}^j \subset \mathbb{R}^n$ and $\frac{\partial h^j(x)}{\partial x} \neq 0$ for any $x \in \partial C_\cap$ where $h^j(x) = 0$, then C_\cap is forward invariant.*

Proof. The proof is the same as that for Proposition 1 of [21], namely $\dot{h}^j(x) = -\alpha(x) \geq 0$ for any j such that $h^j(x) = 0$

so the result follows by Nagumo's Theorem [42]. We add the assumption that $\frac{\partial h^j(x)}{\partial x}$ is non-zero for all $x \in \partial C_\cap$ such that $h^j(x) = 0$ to ensure that the tangent cone in Nagumo's Theorem is non-empty. \square

Then for non-autonomous systems with dynamics (1), we have the following corollary of Theorem 1.

Corollary 1. *Given a dynamical system (1) and a set C_\cap defined by (25) for continuously differentiable functions $h^j : \mathbb{R}^n \rightarrow \mathbb{R}$ where h^j is a ZCBF on D^j and $\frac{\partial h^j(x)}{\partial x} \neq 0$ for any $x \in \partial C_\cap$ where $h^j(x) = 0$, then any Lipschitz continuous controller $u : \mathcal{D}_\cap \rightarrow U$ such that $u(x) \in K_\cap(x)$ will render the set C_\cap forward invariant.*

C. The Shared Nominal Evading Maneuver Assumption

Suppose there are q constraints $\rho^j : \mathcal{D}^j \rightarrow \mathbb{R}$ ($j = 1, \dots, q$) that must be greater than or equal to 0 at all times. For the k agents with pairwise constraints $q = k(k-1)/2$. We assume that for each constraint $j = 1, \dots, q$, a locally Lipschitz nominal evading maneuver γ^j has been selected using the framework in (9). An example for fixed-wing UAVs with collision avoidance safety constraints is given in (13). Given q safety functions ρ^j and evading maneuvers γ^j for $j \in \{1, \dots, q\}$, we construct q output functions h^j defined on \mathcal{D}^j similarly to (9) where

$$h^j(x; \rho, \gamma) = \inf_{\tau \in [0, \infty)} \rho^j(\hat{x}^j(\tau)), \quad (27)$$

$$\hat{x}^j(\tau) = x + \int_0^\tau \hat{\dot{x}}^j(\eta) d\eta, \quad (28)$$

$$\hat{\dot{x}}^j(\tau) = f(\hat{x}^j(\tau)) + g(\hat{x}^j(\tau))\gamma^j(\hat{x}^j(\tau)). \quad (29)$$

Section IV.A showed an example where K_\cap could be empty for some $x \in C_\cap$. As a result, the assumptions of Corollary 1 could not be satisfied. In order to address the issue discussed in Section IV.A, we introduce an additional constraint on γ^j ($j = 1, \dots, q$) that all h^j are constructed from the same nominal evading maneuver.

Assumption 1. Given a dynamical system (1) and q output functions h^j defined in (27) for given safety functions ρ^j and evading maneuvers γ^j for $j \in \{1, \dots, q\}$, the *shared evading maneuver assumption* holds if $\gamma^1(x) = \dots = \gamma^q(x)$ for all $x \in \mathcal{D}_\cap$. The *shared evading maneuver* is denoted γ^s so that

$$\gamma^s(x) = \gamma^1(x) = \dots = \gamma^q(x) \quad (30)$$

for all $x \in \mathcal{D}_\cap$.

Remark 4. This assumption requires that each h^j ($j = 1, \dots, q$) be constructed from the same nominal evading maneuver. Note, however, that this does not imply that each h^j must be constructed from the same safety function.

The example in Section IV.A does not satisfy Assumption 1 because $\gamma^1(x)$ and $\gamma^2(x)$ defined in (21) are not the

same. To enforce that the shared evasive maneuver assumption holds, one option is to change γ^1 so that

$$\gamma^1(x) = \begin{bmatrix} 1 & 1 & 0 & 1 & 1 & 0 & 1 & 1 & 0 \end{bmatrix}^T. \quad (31)$$

In other words, using γ^1 defined in (31) and γ^2 and γ^3 in (20b) implies an evasive maneuver where all vehicles turn left for each constraint. Another example where the shared nominal evading maneuver assumption holds is as follows:

$$\gamma^s(x) = \gamma^1(x) = \gamma^2(x) = \gamma^3(x) = \begin{bmatrix} 1 & 1 & 0 & 1.5 & 0 & 0 & 2 & -1 & 0 \end{bmatrix}^T.$$

In this case, $\gamma^s(x)$ encodes an evasive maneuver where vehicle 1 turns left with a linear velocity of 1, vehicle 2 stays straight with a linear velocity of 1.5, and vehicle 3 turns right with a linear velocity of 2. These three nominal evading maneuvers satisfy the shared evasive maneuver assumption because for all $x \in \mathcal{D}_\cap$, $\gamma^1(x) = \gamma^2(x) = \gamma^3(x)$.

To see the purpose of Assumption 1, we first examine the case of a single constraint. In particular, let h be defined in (9) and consider the role of γ in establishing that h is a ZCBF. From Definition 1, for h to be used for a barrier function, $K(x)$ must be nonempty for all $x \in \mathcal{D}$. With h defined as in (9), this property is satisfied by $\gamma(x)$ or a perturbation of $\gamma(x)$ for all $x \in \mathcal{D}$ (see Theorem 2). The analogue condition for multiple constraints is that $K_\cap(x)$ is non-empty for all $x \in \mathcal{D}_\cap$. If each h^j defined in (9) is a ZCBF and is constructed from γ^j then by similar reasoning to Theorem 2, $\gamma^j(x)$ or a perturbation of $\gamma(x)$ is in $K^j(x)$ for all $x \in \mathcal{D}_\cap$. This allows us to state a multiple constraint analogue to Theorem 2. In the following, we denote the inner product as $\langle L_g h^{j_1}(x), L_g h^{j_2}(x) \rangle$ for $j_1, j_2 \in \{1, \dots, q\}$.

Theorem 3. *Given a dynamical system (1) and a set $C_\cap \subset \mathcal{D}_\cap$ defined in (25) for q continuously differentiable functions h^j defined in (27) with safety functions ρ^j and evading maneuvers γ^j where $k \in \{1, \dots, q\}$, if h^j is a ZCBF for $k \in \{1, \dots, q\}$ and Assumption 1 holds then $K_\cap(x)$ is non-empty for all $x \in C_\cap$. If in addition, γ^s defined in (30) maps to the interior of U and for all $x \in \partial C_\cap$, $\langle L_g h^{j_1}(x), L_g h^{j_2}(x) \rangle > 0$ for $j_1 \neq j_2$ and $j_1, j_2 \in \{1, \dots, q\}$, then there is an open set that is a superset of C_\cap for which $K_\cap(x)$ is non-empty for all x in the open set.*

Proof. To prove the first statement, note that it was shown in the proof of Theorem 2 that γ^s is in $K^j(x)$ for $j = 1, \dots, q$ and $x \in C_\cap$. To prove the second statement, note that we can use the same method as was used in the proof of Theorem 2 to find a vector $d(z)$ such that $h^j(z)$ satisfies (4) for all $z \in B(x, \mu)$ given $x \in \partial C_\cap$. In particular, because $\langle L_g h^{j_1}(x), L_g h^{j_2}(x) \rangle > 0$, $L_g h^j(x) \neq 0$ for $j = 1, \dots, q$ there exists a vector $d_{all}(x)$ such that $\langle d_{all}(x), L_g h^j(x) \rangle > 0$. We choose $d_{all}(x)$ with sufficiently small norm. Using the notation of the proof of Theorem 2, for sufficiently small μ , the projection of $d_{all}(x)$ onto $L_g h(z)$ will be in the direction of $L_g h(z)$ for $z \in B(x, \mu)$ because $L_g h(x)$ is continuous. \square

Remark 5. A geometric view of the problem introduced in Section IV.A and its resolution via the shared evading

maneuver assumption is shown in Figure 5.

Similar to the QP in (6), we write a QP with q constraints and let $\hat{u} = \begin{bmatrix} \hat{u}_1^T & \hat{u}_2^T & \dots & \hat{u}_k^T \end{bmatrix}^T$ where \hat{u}_i is the nominal input of vehicle i for $i = 1, \dots, k$. To emphasize that all h^j are constructed from γ^s , we write $h^{j,s}$ for each $j = 1, \dots, q$ as follows:

$$\begin{aligned} u^* &= \min_{u \in \mathbb{R}^m} \frac{1}{2} \|u - \hat{u}\|^2 \\ \text{s.t.} \quad Au &\geq b. \\ L_f h^{j,s}(x) + L_g h^{j,s}(x)u + \alpha(h^{j,s}(x)) &\geq 0 \quad j \in \{1, \dots, q\}. \end{aligned} \tag{32}$$

V. CONTROL CALCULATION WITH LIMITED COMMUNICATION

The QP in (32) is a centralized calculation. In particular, it requires that each vehicle's nominal control input \hat{u}_i be communicated. Frequently communicating this signal when there are many vehicles may reduce throughput for other important messages or introduce communication delays because a network can only support a limited number of bits per second through a network. Thus, we show how to ensure safety constraints can be satisfied by reformulating the QP so that the vehicles can calculate a safe control signal without requiring each other's nominal control input.

We start by considering the two vehicle case and then generalize to the k vehicle case. Let $\gamma^s = \begin{bmatrix} \gamma_1^{sT} & \gamma_2^{sT} \end{bmatrix}^T$ be the shared evading maneuver where γ_1^{sT} is the part of γ^s that is applied to vehicle 1 and therefore has the same size as u_1 . Define γ_2^s similarly for vehicle 2. Similarly decompose b in (6c) as $b = \begin{bmatrix} b_1^T & b_2^T \end{bmatrix}^T$ and $L_g h^{j,s}(x)$ as $L_g h^{j,s}(x) = \begin{bmatrix} [L_g h^{j,s}(x)]_1^T & [L_g h^{j,s}(x)]_2^T \end{bmatrix}^T$. Further, let A in (6c) be block diagonal with block entries A_1 and A_2 so that $A_i u_i \geq b_i$ represents the actuator constraint for vehicle i for $i = 1, 2$.

We want to find a way of calculating u_1 and u_2 such that $u = \begin{bmatrix} u_1^T & u_2^T \end{bmatrix}^T$ satisfies $Au \geq b$ and $u \in K^j(x)$ for all $x \in \mathcal{D}$ where the calculation for u_1 does not require knowledge of \hat{u}_2 or the final value for u_2 . Similarly, we want to calculate u_2 without knowledge of \hat{u}_1 or u_1 . This is a trivial requirement for actuator constraints since $A_i u_i \geq b_i$ for $i = 1, 2$ if and only if $Au \geq b$. However, the constraint that $u \in K_\cap(x)$ involves both u_1 and u_2 so we reformulate it as follows:

$$\begin{aligned} 0 &\leq L_f h^{j,s}(x) + L_g h^{j,s}(x)u + \alpha(h^{j,s}(x)) \\ &= \kappa_1(x, u_1) + \kappa_2(x, u_2) \end{aligned}$$

where

$$\kappa_1(x, u_1) = L_f h^{j,s}(x) + [L_g h^{j,s}(x)]_1 u_1 + \alpha(h^{j,s}(x)) + [L_g h^{j,s}(x)]_2 \gamma_2^s - \frac{1}{2} (L_f h^{j,s}(x) + L_g h^{j,s}(x) \gamma^s + \alpha(h^{j,s}(x)))$$

and

$$\kappa_2(x, u_2) = L_f h^{j,s}(x) + [L_g h^{j,s}(x)]_2 u_2 + \alpha(h^{j,s}(x)) + [L_g h^{j,s}(x)]_1 \gamma_1^s - \frac{1}{2}(L_f h^{j,s}(x) + L_g h^{j,s}(x) \gamma^s + \alpha(h^{j,s}(x))).$$

Notice that κ_1 is not a function of u_2 and κ_2 is not a function of u_1 . In other words, if we can select u_1 and u_2 such that $\kappa_1(x, u_1) \geq 0$ and $\kappa_2(x, u_2) \geq 0$ then $u = \begin{bmatrix} u_1^T & u_2^T \end{bmatrix}^T \in K_\cap(x) \forall x \in C$. For $x \in C_\cap$, this can be done by letting $u_1 = \gamma_1^s(x)$ and $u_2 = \gamma_2^s(x)$ and noting that this implies

$$\kappa_1(x, \gamma_1^s) + \kappa_2(x, \gamma_2^s) = L_f h^{j,s}(x) + L_g h^{j,s}(x) \gamma^s + \alpha(h^{j,s}(x)) \geq 0.$$

For $x \notin C_\cap$, a perturbation of $\gamma_1^s(x)$ and $\gamma_2^s(x)$ using a similar method as shown in the proof of Theorem 3 suffices. In other words, we can find u without vehicle 1 needing to know \hat{u}_2 or u_2 and similarly for vehicle 2. Each vehicle i ($i = 1, 2$) could then calculate the following QP:

$$\begin{aligned} u^* &= \min_{u \in \mathbb{R}^{m_i}} \frac{1}{2} \|u - \hat{u}_i\|^2 & (33) \\ \text{s.t.} \quad & A_i u_i \geq b_i \\ & \kappa_i(x, u_i) \geq 0. \end{aligned}$$

Note that $\kappa_i(x, u_i)$ is linear in u_i .

We now generalize the above discussion to k vehicles. Let $\gamma^s = \begin{bmatrix} \gamma_1^{sT} & \dots & \gamma_k^{sT} \end{bmatrix}^T$, where γ_i^s maps to vectors of the same size as u_i for $i = 1, \dots, k$ with similar decomposition for $b = \begin{bmatrix} b_1^T & \dots & b_k^T \end{bmatrix}^T$ and $L_g h^{j,s}(x) = \begin{bmatrix} [L_g h^{j,s}(x)]_1^T & \dots & [L_g h^{j,s}(x)]_k^T \end{bmatrix}^T$. Further, assume A in (6c) is block diagonal with block entries A_i for $i = 1, \dots, k$ where A_i is a $m_i \times m_i$ matrix. This assumption means that actuator constraints are not coupled between vehicles. For constraint j for $j = 1, \dots, q$, let

$$\mathcal{V}^j = \{i \in \{1, \dots, k\} : \exists x \in \mathcal{D} \text{ s.t. } [L_g h^{j,s}(x)]_i \neq 0_{m_i}\}$$

where 0_{m_i} is the zero vector in \mathbb{R}^{m_i} . \mathcal{V}^j represents the set of vehicles whose control input affects the time derivative of h^j for some $x \in \mathcal{D}$. We let $|\mathcal{V}^j|$ denote the cardinality of \mathcal{V}^j , and note that for the case of pairwise collision avoidance, $|\mathcal{V}^j| = 2$ for all $j = 1, \dots, q$. In the example with three vehicles in Section IV, $\mathcal{V}_1 = \{1, 2\}$, $\mathcal{V}_2 = \{1, 3\}$, $\mathcal{V}_3 = \{2, 3\}$. Finally, we denote $u_{\setminus i} = \begin{bmatrix} u_1^T & \dots & u_{i-1}^T & u_{i+1}^T & \dots & u_k^T \end{bmatrix}^T$, with similar definitions for $\gamma_{\setminus i}^s$, $\hat{u}_{\setminus i}$, and $[L_g h^{j,s}(x)]_{\setminus i}$.

With the above definitions, we can now state a limited communication analogue for the admissible control space in (5). The limited communication admissible control space for constraint j ($j = 1, \dots, q$) and vehicle i ($i \in \mathcal{V}^j$) is

defined as

$$\mathcal{K}_i^j(x) = \left\{ u_i \in U_i : 0 \leq L_f h^{j,s}(x) + [L_g h^{j,s}(x)]_i u_i + \alpha(h^{j,s}(x)) + [L_g h^{j,s}(x)]_{\setminus i} \gamma_{\setminus i}^s(x) - \frac{|\mathcal{V}^j| - 1}{|\mathcal{V}^j|} \left(L_f h^{j,s}(x) + L_g h^{j,s}(x) \gamma^s(x) + \alpha(h^{j,s}(x)) \right) \right\}.$$

Let $\mathcal{S}_i = \{j \in \{1, \dots, q\} : i \in \mathcal{V}^j\}$ so that \mathcal{S}_i is the set of safety constraint indices where u_i has an effect on the time derivative of the associated barrier function for some $x \in \mathcal{D}$. For the three vehicle example of Section IV, $\mathcal{S}_1 = \{1, 2\}$, $\mathcal{S}_2 = \{1, 3\}$, $\mathcal{S}_3 = \{2, 3\}$. The limited communication admissible control space for vehicle i is then $\mathcal{K}_i(x) = \bigcap_{l \in \mathcal{S}_i} \mathcal{K}_i^l(x)$ and the overall limited communication admissible control space is

$$\mathcal{K}(x) = \left\{ u = \begin{bmatrix} u_1^T & \dots & u_k^T \end{bmatrix}^T \in U : u_i \in \mathcal{K}_i(x) \forall i \in \{1, \dots, k\} \right\}.$$

Theorem 4. *Given a dynamical system (1) and a set $C_\cap \subset \mathcal{D}_\cap$ defined in (25) for q continuously differentiable functions h^j defined in (27) with safety functions ρ^j and evading maneuvers γ^j where $k \in \{1, \dots, q\}$, if h^j is a ZCBF for $k \in \{1, \dots, q\}$ and Assumption 1 holds then $\forall x \in \mathcal{D}_\cap$, $\mathcal{K}(x) \subseteq K_\cap(x)$. Further, $\mathcal{K}(x)$ is non-empty for all $x \in C_\cap$. If in addition, γ^s maps to the interior of U and for all $x \in \partial C_\cap$, $\langle [L_g h^{j_1}(x)]_i, [L_g h^{j_2}(x)]_i \rangle > 0$ for $j = 1, \dots, q$ and $i = 1, \dots, k$ and $j_1 \neq j_2$ and $j_1, j_2 \in \{1, \dots, q\}$, then there is an open set that is a superset of C_\cap for which $\mathcal{K}(x)$ is non-empty for all x in the open set.*

Proof. For the first statement, assume $u \in \mathcal{K}(x)$ so that $u_i \in \mathcal{K}_i(x) \forall i \in \{1, \dots, k\}$. This means that $A_i u_i \geq b_i$ so that, because A is block diagonal, $Au \geq b$. Further, it means that for any constraint $j = 1, \dots, q$ and any $i \in \mathcal{V}^j$,

$$0 \leq L_f h^{j,s}(x) + [L_g h^{j,s}(x)]_i u_i + \alpha(h^{j,s}(x)) + [L_g h^{j,s}(x)]_{\setminus i} \gamma_{\setminus i}^s(x) - \frac{|\mathcal{V}^j| - 1}{|\mathcal{V}^j|} \left(L_f h^{j,s}(x) + L_g h^{j,s}(x) \gamma^s(x) + \alpha(h^{j,s}(x)) \right). \quad (34)$$

To simplify (34), note that by definition, $[L_g h^{j,s}(x)]_i = 0_{m_i}$ for $i \notin \mathcal{V}^j$ so that

$$\begin{aligned} \sum_{i \in \mathcal{V}^j} [L_g h^{j,s}(x)]_i u_i &= \sum_{i \in \{1, \dots, k\}} [L_g h^{j,s}(x)]_i u_i \\ &= L_g h^{j,s}(x) u. \end{aligned} \quad (35)$$

Using (35) in the following then yields

$$\begin{aligned}
\sum_{i \in \mathcal{V}^j} [L_g h^{j,s}(x)]_{\setminus i} \gamma_{\setminus i}^s(x) &= \sum_{i \in \mathcal{V}^j} (L_g h^{j,s}(x) \gamma^s(x) - [L_g h^{j,s}(x)]_i \gamma_i^s(x)) \\
&= |\mathcal{V}^j| L_g h^{j,s}(x) \gamma^s(x) - \sum_{i \in \mathcal{V}^j} [L_g h^{j,s}(x)]_i \gamma_i^s(x) \\
&= |\mathcal{V}^j| L_g h^{j,s}(x) \gamma^s(x) - L_g h^{j,s}(x) \gamma^s(x) \\
&= (|\mathcal{V}^j| - 1) L_g h^{j,s}(x) \gamma^s(x). \tag{36}
\end{aligned}$$

Summing (34) over $i \in \mathcal{V}^j$ and using (35) and (36) yields

$$\begin{aligned}
0 &\leq |\mathcal{V}^j| L_f h^{j,s}(x) + L_g h^{j,s}(x) u + |\mathcal{V}^j| \alpha(h^{j,s}(x)) + (|\mathcal{V}^j| - 1) L_g h^{j,s}(x) \gamma^s(x) \\
&\quad - (|\mathcal{V}^j| - 1) \left(L_f h^{j,s}(x) + L_g h^{j,s}(x) \gamma^s(x) + \alpha(h^{j,s}(x)) \right) \\
&= L_f h^{j,s}(x) + L_g h^{j,s}(x) u + \alpha(h^{j,s}(x)).
\end{aligned}$$

Since this is true for all $j = 1, \dots, q$, $u \in K_\cap(x)$. Then $\mathcal{K}(x) \subseteq K_\cap(x)$ for all $x \in C_\cap$.

Consider now the second statement, namely that $\gamma^s \in \mathcal{K}(x)$. For $j = 1, \dots, q$, consider any $i \in \mathcal{V}^j$ and let $u_i = \gamma_i^s$.

Then

$$\begin{aligned}
&L_f h^{j,s}(x) + [L_g h^{j,s}(x)]_i u_i + \alpha(h^{j,s}(x)) + [L_g h^{j,s}(x)]_{\setminus i} \gamma_{\setminus i}^s(x) - \frac{|\mathcal{V}^j| - 1}{|\mathcal{V}^j|} \left(L_f h^{j,s}(x) + L_g h^{j,s}(x) \gamma^s(x) + \alpha(h^{j,s}(x)) \right) \\
&= \frac{1}{|\mathcal{V}^j|} \left(L_f h^j(x) + L_g h^j(x) \gamma^s(x) + \alpha(h^j(x)) \right) \\
&\geq 0.
\end{aligned}$$

The inequality is true because $x \in C_\cap$ implies $\alpha(h^{j,s}(x)) \geq 0$. See the proof for Theorem 2 for why $L_f h^{j,s}(x) + L_g h^{j,s}(x) \gamma^s(x) \geq 0$. Then $\gamma_i^s \in \mathcal{K}_i^j$ for any $j = 1, \dots, q$ and $i \in \mathcal{V}^j$. Then $\gamma_i^s \in \mathcal{K}_i$. Then $\gamma^s(x) \in \mathcal{K}(x)$.

Finally, the last statement where $\mathcal{K}(x)$ is nonempty for all x in an open set that is a superset of C_\cap follows similarly to the proof of Theorem 3. \square

We now write a QP similar to (32) but without requiring knowledge of other agents' low level control values as

follows:

$$\begin{aligned}
u_i^* &= \min_{u_i \in \mathbb{R}^{m_i}} \frac{1}{2} \|u_i - \hat{u}_i\|^2 \\
\text{s.t. } & A_i u_i \geq b_i \\
& L_f h^{j,s}(x) + [L_g h^{j,s}(x)]_i u_i + \alpha(h^{j,s}(x)) + [L_g h^{j,s}(x)]_{\setminus i} \gamma_{\setminus i}^s(x) \\
& \quad - \frac{|\mathcal{V}^j| - 1}{|\mathcal{V}^j|} \left(L_f h^{j,s}(x) + L_g h^{j,s}(x) \gamma^s(x) + \alpha(h^{j,s}(x)) \right) \geq 0 \quad j \in \mathcal{S}_i.
\end{aligned} \tag{37}$$

We note that the solution from the centralized QP (32) may be different than the solution from the limited communication QPs (37) because $\mathcal{K}(x)$ may be a strict subset of $K_{\cap}(x)$. To see this, let $k = 2$, $q = 1$, $L_f h(x) = 0$, $\alpha(h(x)) = 0$, $m_1 = m_2 = 1$, $[L_g h(x)]_2 \gamma_2^s(x) = -1$, and $[L_g h(x)]_1 \gamma_1^s(x) = 1$. Then the barrier function constraint in (37) becomes $[L_g h(x)]_1 u_1 \geq 1$, while the barrier function constraint in (32) becomes $L_g h(x) u \geq 0$. Since $u_1 = 0$ is feasible for the latter but not the former equation, we do not have that $\mathcal{K}(x) = K_{\cap}(x)$. Because $\mathcal{K}(x) \subset K_{\cap}(x)$, it may be that the total cost of each vehicle calculating (37) is higher than the centralized calculation (32). In other words, the calculated safe control may not be as close to the nominal control signal in a least squares sense when using (37) as opposed to (32). Nevertheless, in either case of (32) or (37), a solution exists to the corresponding QP such that $u \in K_{\cap}$.

Another difference between the limited communication (37) and the centralized (32) QPs is how the size of the optimization variable and number of constraints vary with the number of vehicles k . In the centralized approach (32) the size of the optimization variable grows linearly with k while the number of constraints grows quadratically. On the other hand, in the limited communication QP (37), the size of the optimization variable and number of constraints are constant and linear, respectively.

VI. SIMULATION

In this section we repeat the scenario discussed in Section III.D but consider $k = 20$ vehicles. For the scenario where h is constructed from γ_{turn} , we use $\begin{bmatrix} v & \omega & 0 & v & \omega & 0 \end{bmatrix}^T$ where $v = 0.9v_{min} + 0.1v_{max}$ and $\omega = 0.9\omega_{max}$. For the scenario where h is constructed from $\gamma_{straight}$, we let $\gamma^i = \begin{bmatrix} (1 + 0.01i)v & 0 & 0 \end{bmatrix}^T$ so that each vehicle uses a different translational velocity as is required to ensure differentiability of h (see Section III.C). Note that this does not violate the shared evading maneuver assumption because $\gamma^s = \begin{bmatrix} (\gamma^1)^T & \dots & (\gamma^k)^T \end{bmatrix}^T$. Additionally, we let $\psi = 0$ and $\psi = 25^\circ$ in the scenario where h is constructed from γ_{turn} and $\gamma_{straight}$, respectively. Offsetting the initial orientation 25° from pointing at the origin is required so that the vehicles can start in the safe set when using $\gamma_{straight}$. Screenshots for the case of γ_{turn} and $\gamma_{straight}$ are shown in Figures 6 and 7, respectively. Quantitative results for both scenarios are shown in Figure 8 which shows similar outputs to the results for the two vehicle simulation shown in Figure 2. In

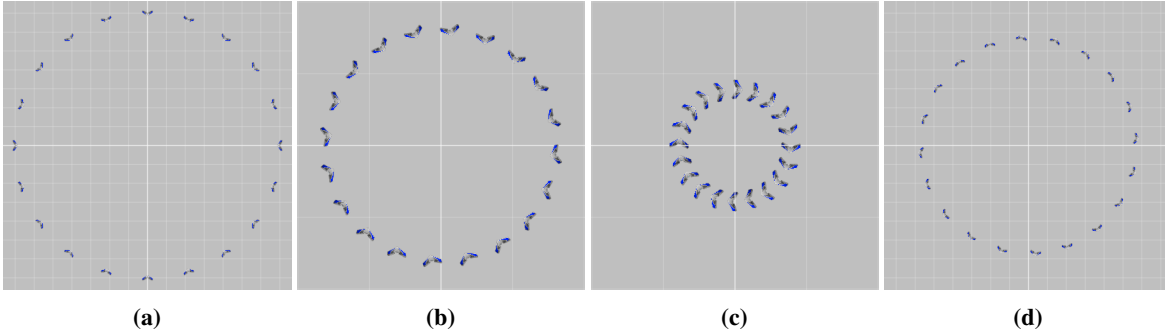


Fig. 6 A demonstration of 20 fixed-wing vehicles applying barrier functions to ensure collisions are avoided when constructing h defined in (9) by γ_{turn} . (a) The starting position of 20 vehicles. (b) The vehicles approach the origin and begin avoidance behavior around 50 meters away from the origin. (c) The vehicles circle the origin. (d) The vehicles reach approach their target position.

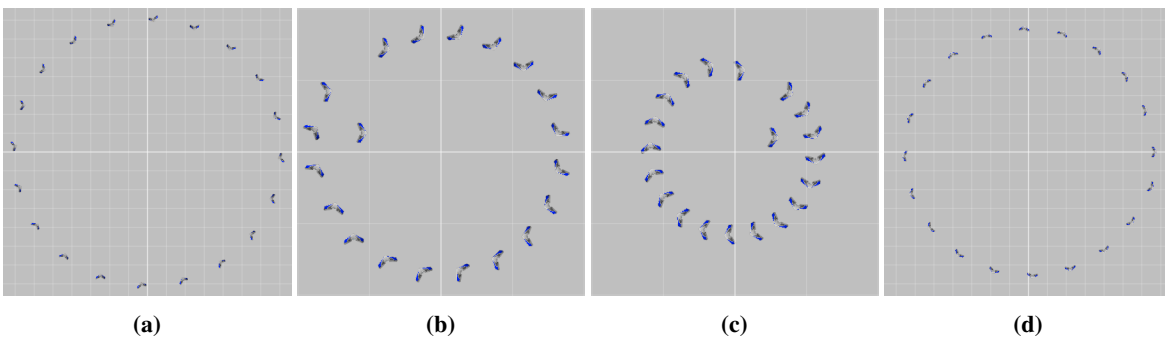


Fig. 7 A demonstration of 20 fixed-wing vehicles applying barrier functions to ensure collisions are avoided when constructing h defined in (9) by $\gamma_{straight}$. (a) The starting position of 20 vehicles. (b) The vehicles approach the origin and begin avoidance behavior around 50 meters away from the origin. (c) The vehicles circle the origin. (d) The vehicles reach approach their target position. The asymmetry is due to the fact that the vehicles have different speeds for their nominal evading maneuvers. As the speed for the nominal maneuvers approaches the same value the result is a more symmetric pattern.

particular, the pairwise distance between all vehicles are kept above the minimum safety distance D_s while satisfying actuator constraints.

VII. CONCLUSION

In this paper we have examined method for ensuring a system with constrained inputs can be safe for all future times. The main result is a general method for constructing a barrier function given a safety constraint, system dynamics with actuator limits, and an evasive function specified by a safety engineer. We then apply this method to show how collision avoidance for two UAVs can be ensured for all future times. The result is then extended to the case of collision avoidance for arbitrarily many UAVs by considering how to ensure that arbitrarily many safety objectives can be satisfied simultaneously. In the case of arbitrarily many UAVs, network constraints may limit the message throughput so we provide a reformulation of the algorithm that requires less message passing while still ensuring that vehicles will stay safe. The final result is demonstrated in a simulation of 20 UAVs where the vehicles are on a collision course. However,

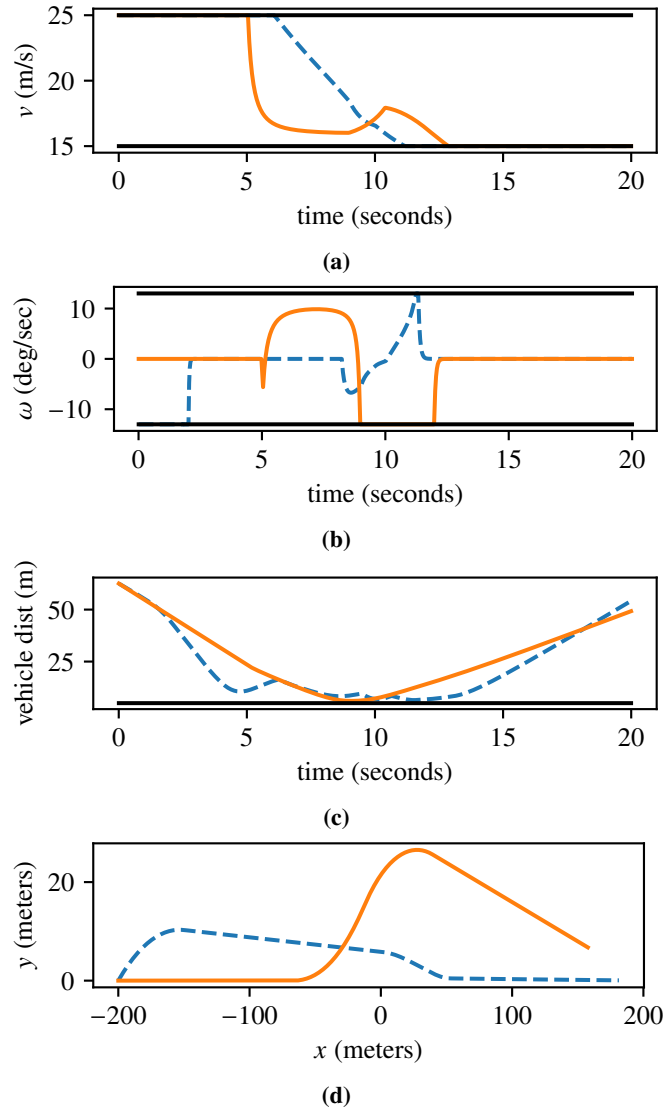


Fig. 8 Outputs for the scenario with 20 fixed-wing vehicles. The blue dashed and orange solid lines are the output of the scenario where h is constructed from $\gamma_{straight}$ and γ_{turn} , respectively. Vehicle 1 velocity and turn rates are shown to be within the actuator limits in (a) and (b). Vehicle 1 is plotted as a representative output since all 20 vehicles cannot be shown on the same plot. In (c), the minimum distance between any two vehicles is shown to be above D_s . (d) is the path taken by vehicle 1. Note that the behavior is significantly different when constructing h with γ_{turn} and $\gamma_{straight}$.

due to the role of the barrier function in ensuring safety, all twenty vehicles nevertheless maintain safe distances from each other and then able to reach their assigned waypoints.

Appendix

An Analysis of The Role of δ in The Continuous Differentiability of h_{turn}

Note that (16) is not necessarily differentiable when $A_2 = 0$ since A_2 results from a square root performed in phasor addition. Thus, in this section, we consider how to ensure A_2 is continuously differentiable to ensure h in (16) is continuously differentiable. Consider (16) in phasor form

$$\begin{aligned} A_1 - D_s^2 + A_2 e^{j\Theta} &= A_1 - D_s^2 + \sigma A_3 e^{j(\theta_{1,0}-\pi/2)} + A_3 e^{j(\theta_{2,0}+\pi/2)} + \delta e^{j(\theta_{1,0}-\pi/2)} \\ &\quad + \sigma A_4 e^{j(\theta_{1,0}-\pi)} + A_4 e^{j\theta_{2,0}} + \delta e^{j(\theta_{1,0}-\pi)} \\ &= A_1 - D_s^2 + A_5 e^{j\Theta_5} + A_6 e^{j\Theta_6} \end{aligned} \quad (38)$$

where $A_3 = 2\Delta b_0 r$, $A_4 = 2\Delta c_0 r$, $A_5 e^{j\Theta_5} = \sigma A_3 e^{j(\theta_{1,0}-\pi/2)} + A_3 e^{j(\theta_{2,0}+\pi/2)} + \delta e^{j(\theta_{1,0}-\pi/2)}$, and $A_6 e^{j\Theta_6} = \sigma A_4 e^{j(\theta_{1,0}-\pi)} + A_4 e^{j\theta_{2,0}} + \delta e^{j(\theta_{1,0}-\pi)}$. Notice that $\Theta_5 - \Theta_6 = \pi/2$. In other words, A_2 is zero only when both A_5 and A_6 are zero. For $\delta = 0$, A_5 and A_6 are both zero on the set $Z_1 \subseteq \mathcal{D}$ where $\theta_{1,0} = \theta_{2,0}$ or $\theta_{1,0} = \theta_{2,0} + \pi$. Although Z_1 is a zero measure set, we note that for $\delta > 0$ that A_2 is zero on a set $Z_2 \subset Z_1$ where Z_2 is the restriction of Z_1 to a specific set of positions which we now specify.

Case 1. Vehicles Start in Opposite Directions. Suppose $\theta_{1,0} = \theta_{2,0} + \pi$. Then $A_5 = 0$ when $\delta = -(1 + \sigma)A_3 = -2(1 + \sigma)\Delta b_0 r$. Similarly, $A_6 = 0$ when $\delta = -(1 + \sigma)A_4 = -2(1 + \sigma)\Delta c_0 r$. Suppose δ is fixed. Then $A_2 = 0$ when $-\frac{\delta}{2(1+\sigma)r} = \Delta b_0 = p_{1,x_0} - p_{2,x_0} + r(1 + \sigma) \sin \theta_{2,0}$ and $-\frac{\delta}{2(1+\sigma)r} = \Delta c_0 = p_{1,y_0} - p_{2,y_0} - r(1 + \sigma) \cos \theta_{2,0}$.

Case 2. Vehicles Start in the Same Direction. Suppose $\theta_{1,0} = \theta_{2,0}$. Then $A_5 = 0$ when $\delta = (1 - \sigma)A_3$. Similarly, $A_6 = 0$ when $\delta = (1 - \sigma)A_4$. For $\sigma = 1$, let $\delta > 0$ to ensure A_5 and A_6 are not simultaneously 0. For $0 < \sigma < 1$, a similar analysis to the previous case implies $A_2 = 0$ when when $-\frac{\delta}{2(1-\sigma)r} = \Delta b_0 = p_{1,x_0} + p_{2,x_0} - r(1 - \sigma) \sin \theta_{2,0}$ and $-\frac{\delta}{2(1-\sigma)r} = \Delta c_0 = p_{1,y_0} - p_{2,y_0} - r(1 + \sigma) \cos \theta_{2,0}$.

An Analysis of the Continuous Differentiability of $h_{straight}$

From (19) we expand terms to get

$$h(x) = \inf_{\tau \in [0, \infty)} c(x) + b(x)\tau + a(x)\tau^2 \quad (39)$$

where $c(x) = \Delta x^2 + \Delta y^2 + \Delta z^2 - D_s^2$, $b(x) = 2(\Delta x \Delta C + \Delta y \Delta S)$, $a(x) = \Delta C^2 + \Delta S^2$, $\Delta x = p_{1,x_0} - p_{2,x_0}$, $\Delta y = p_{1,y_0} - p_{2,y_0}$, $\Delta z = p_{1,z_0} - p_{2,z_0}$, $\Delta C = v_1 \cos \theta_1 - v_2 \cos \theta_2$, $\Delta S = v_1 \sin \theta_1 - v_2 \sin \theta_2$. We also note that $a(x) > 0$ since

$$\begin{aligned}
a(x) &= (v_1 \cos \theta_1 - v_2 \cos \theta_2)^2 + (v_1 \sin \theta_1 - v_2 \sin \theta_2)^2 \\
&= v_1^2 + v_2^2 - 2v_1 v_2 \cos(\theta_1 - \theta_2) \\
&= v_1^2 + v_2^2 - 2v_1 v_2 + 2v_1 v_2 - 2v_1 v_2 \cos(\theta_1 - \theta_2) \\
&= (v_1 - v_2)^2 + 2v_1 v_2(1 - \cos(\theta_1 - \theta_2)) \\
&> 0
\end{aligned}$$

since $v_1 \neq v_2$ and v_1 and v_2 are positive. Then $\tau_{min}(x) = -b(x)/2a(x)$ is well defined. Then h has a minimum at $\tau_{nonneg,min} = \max(0, \tau_{min}(x))$.

For $\tau_{nonneg,min}(x) > 0$, h is continuously differentiable because c , b , τ_{min} , and a are continuously differentiable. Consider now when $\tau_{nonneg,min}(x) = 0$. We verify that $\frac{\partial h(x)}{\partial x} = \frac{\partial c(x)}{\partial x}$ for either the case of $\tau_{min} = 0$ or $\tau_{min} = -b(x)/2a(x)$. In the first case, $h(x) = c(x)$ and $\frac{\partial h(x)}{\partial x} = \frac{\partial c(x)}{\partial x}$. In the second case, $h(x) = c(x) + b(x)\tau_{min} + a(x)\tau_{min}^2$ and

$$\begin{aligned}
\frac{\partial h(x)}{\partial x} &= \frac{\partial c(x)}{\partial x} + \frac{\partial b(x)}{\partial x} \tau_{min}(x) + b(x) \frac{\partial \tau_{min}(x)}{\partial x} + \frac{\partial a(x)}{\partial x} \tau_{min}(x) + 2a(x) \tau_{min} \frac{\partial \tau_{min}(x)}{\partial x} \\
&= \frac{\partial c(x)}{\partial x}
\end{aligned}$$

because in this case $b(x)$ and $\tau_{min}(x)$ are 0.

Funding Sources

The work of Eric Squires was supported by the University System of Georgia's Tuition Assistance Program. The work by Magnus Egerstedt and Pietro Pierpaoli was supported by Grant No. ARL DCIST CRA W911NF-17-2-0181 by the US Army Research Lab. The work of Samuel Coogan and Rohit Konda was supported by the Air Force Office of Scientific Research under grant number FA9550-19-1-0015.

References

- [1] Prevot, T., Rios, J., Kopardekar, P., Robinson III, J. E., Johnson, M., and Jung, J., "UAS traffic management (UTM) concept of operations to safely enable low altitude flight operations," *16th AIAA Aviation Technology, Integration, and Operations Conference*, 2016, p. 3292.
- [2] Temizer, S., Kochenderfer, M., Kaelbling, L., Lozano-Pérez, T., and Kuchar, J., "Collision avoidance for unmanned aircraft using Markov decision processes," *AIAA guidance, navigation, and control conference*, 2010, p. 8040.

- [3] Wolf, T. B., and Kochenderfer, M. J., "Aircraft collision avoidance using Monte Carlo real-time belief space search," *Journal of Intelligent & Robotic Systems*, Vol. 64, No. 2, 2011, pp. 277–298.
- [4] Fox, D., Burgard, W., and Thrun, S., "The dynamic window approach to collision avoidance," *IEEE Robotics & Automation Magazine*, Vol. 4, No. 1, 1997, pp. 23–33.
- [5] Seder, M., and Petrovic, I., "Dynamic window based approach to mobile robot motion control in the presence of moving obstacles," *Robotics and Automation, 2007 IEEE International Conference on*, IEEE, 2007, pp. 1986–1991.
- [6] Lalish, E., Morgansen, K. A., and Tsukamaki, T., "Decentralized reactive collision avoidance for multiple unicycle-type vehicles," *American Control Conference, 2008*, IEEE, 2008, pp. 5055–5061.
- [7] Mastellone, S., Stipanović, D. M., Graunke, C. R., Intlekofer, K. A., and Spong, M. W., "Formation control and collision avoidance for multi-agent non-holonomic systems: Theory and experiments," *The International Journal of Robotics Research*, Vol. 27, No. 1, 2008, pp. 107–126.
- [8] Rodriguez-Seda, E. J., "Decentralized trajectory tracking with collision avoidance control for teams of unmanned vehicles with constant speed," *American Control Conference (ACC), 2014*, IEEE, 2014, pp. 1216–1223.
- [9] Panyakeow, P., and Mesbahi, M., "Decentralized deconfliction algorithms for unicycle UAVs," *American Control Conference (ACC), 2010*, IEEE, 2010, pp. 794–799.
- [10] Di, B., Zhou, R., and Duan, H., "Potential field based receding horizon motion planning for centrality-aware multiple UAV cooperative surveillance," *Aerospace Science and Technology*, Vol. 46, 2015, pp. 386–397.
- [11] Defoort, M., Kokosy, A., Floquet, T., Perruquetti, W., and Palos, J., "Motion planning for cooperative unicycle-type mobile robots with limited sensing ranges: A distributed receding horizon approach," *Robotics and autonomous systems*, Vol. 57, No. 11, 2009, pp. 1094–1106.
- [12] Shin, J., and Kim, H. J., "Nonlinear model predictive formation flight," *IEEE Transactions on Systems, Man, and Cybernetics-Part A: Systems and Humans*, Vol. 39, No. 5, 2009, pp. 1116–1125.
- [13] Tomlin, C., Pappas, G. J., and Sastry, S., "Conflict resolution for air traffic management: A study in multiagent hybrid systems," *IEEE Transactions on automatic control*, Vol. 43, No. 4, 1998, pp. 509–521.
- [14] Lai, C.-K., Lone, M., Thomas, P., Whidborne, J., and Cooke, A., "On-board trajectory generation for collision avoidance in unmanned aerial vehicles," *Aerospace Conference, 2011 IEEE*, IEEE, 2011, pp. 1–14.
- [15] Lin, Y., and Saripalli, S., "Path planning using 3D dubins curve for unmanned aerial vehicles," *Unmanned Aircraft Systems (ICUAS), 2014 International Conference on*, IEEE, 2014, pp. 296–304.
- [16] Lin, Y., and Saripalli, S., "Collision avoidance for UAVs using reachable sets," *Unmanned Aircraft Systems (ICUAS), 2015 International Conference on*, IEEE, 2015, pp. 226–235.

- [17] Althoff, D., Althoff, M., and Scherer, S., “Online safety verification of trajectories for unmanned flight with offline computed robust invariant sets,” *2015 IEEE/RSJ International Conference on Intelligent Robots and Systems (IROS)*, IEEE, 2015, pp. 3470–3477.
- [18] Pallottino, L., Scordio, V. G., Bicchi, A., and Frazzoli, E., “Decentralized cooperative policy for conflict resolution in multivehicle systems,” *IEEE Transactions on Robotics*, Vol. 23, No. 6, 2007, pp. 1170–1183.
- [19] Krontiris, A., and Bekris, K. E., “Using minimal communication to improve decentralized conflict resolution for non-holonomic vehicles,” *Intelligent Robots and Systems (IROS), 2011 IEEE/RSJ International Conference on*, IEEE, 2011, pp. 3235–3240.
- [20] Prajna, S., “Barrier certificates for nonlinear model validation,” *Automatica*, Vol. 42, No. 1, 2006, pp. 117–126.
- [21] Ames, A. D., Xu, X., Grizzle, J. W., and Tabuada, P., “Control barrier function based quadratic programs for safety critical systems,” *IEEE Transactions on Automatic Control*, Vol. 62, No. 8, 2017, pp. 3861–3876.
- [22] Borrmann, U., Wang, L., Ames, A. D., and Egerstedt, M., “Control barrier certificates for safe swarm behavior,” *IFAC-PapersOnLine*, Vol. 48, No. 27, 2015, pp. 68–73.
- [23] Wang, L., Ames, A. D., and Egerstedt, M., “Safe certificate-based maneuvers for teams of quadrotors using differential flatness,” *arXiv preprint arXiv:1702.01075*, 2017.
- [24] Nguyen, Q., and Sreenath, K., “Safety-critical control for dynamical bipedal walking with precise footstep placement,” *IFAC-PapersOnLine*, Vol. 48, No. 27, 2015, pp. 147–154.
- [25] Hsu, S.-C., Xu, X., and Ames, A. D., “Control barrier function based quadratic programs with application to bipedal robotic walking,” *American Control Conference (ACC), 2015*, IEEE, 2015, pp. 4542–4548.
- [26] Xu, X., Grizzle, J. W., Tabuada, P., and Ames, A. D., “Correctness guarantees for the composition of lane keeping and adaptive cruise control,” *IEEE Transactions on Automation Science and Engineering*, 2017.
- [27] Xu, X., Tabuada, P., Grizzle, J. W., and Ames, A. D., “Robustness of control barrier functions for safety critical control,” *IFAC-PapersOnLine*, Vol. 48, No. 27, 2015, pp. 54–61.
- [28] Xu, X., Waters, T., Pickem, D., Glotfelter, P., Egerstedt, M., Tabuada, P., Grizzle, J. W., and Ames, A. D., “Realizing simultaneous lane keeping and adaptive speed regulation on accessible mobile robot testbeds,” *Control Technology and Applications (CCTA), 2017 IEEE Conference on*, IEEE, 2017, pp. 1769–1775.
- [29] Wang, L., Ames, A. D., and Egerstedt, M., “Multi-objective compositions for collision-free connectivity maintenance in teams of mobile robots,” *Decision and Control (CDC), 2016 IEEE 55th Conference on*, IEEE, 2016, pp. 2659–2664.
- [30] Prajna, S., and Jadbabaie, A., “Safety verification of hybrid systems using barrier certificates,” *HSCC*, Vol. 2993, Springer, 2004, pp. 477–492.

- [31] Wang, L., Han, D., and Egerstedt, M., “Permissive barrier certificates for safe stabilization using sum-of-squares,” *arXiv preprint arXiv:1802.08917*, 2018.
- [32] Parrilo, P. A., “Semidefinite programming relaxations for semialgebraic problems,” *Mathematical programming*, Vol. 96, No. 2, 2003, pp. 293–320.
- [33] Nguyen, Q., and Sreenath, K., “Exponential control barrier functions for enforcing high relative-degree safety-critical constraints,” *American Control Conference (ACC), 2016*, IEEE, 2016, pp. 322–328.
- [34] Xu, X., “Constrained control of input–output linearizable systems using control sharing barrier functions,” *Automatica*, Vol. 87, 2018, pp. 195–201.
- [35] Gurriet, T., Mote, M., Ames, A. D., and Feron, E., “An online approach to active set invariance,” *2018 IEEE Conference on Decision and Control (CDC)*, IEEE, 2018, pp. 3592–3599.
- [36] Glotfelter, P., Cortés, J., and Egerstedt, M., “Nonsmooth Barrier Functions With Applications to Multi-Robot Systems,” *IEEE control systems letters*, Vol. 1, No. 2, 2017, pp. 310–315.
- [37] Squires, E., Pierpaoli, P., and Egerstedt, M., “Constructive barrier certificates with applications to fixed-wing aircraft collision avoidance,” *2018 IEEE Conference on Control Technology and Applications (CCTA)*, IEEE, 2018, pp. 1656–1661.
- [38] DeMarco, K., Squires, E., Day, M., and Pippin, C., “Simulating collaborative robots in a massive multi-agent game environment (SCRIMMAGE),” *Distributed Autonomous Robotic Systems*, Springer, 2019, pp. 283–297.
- [39] Olfati-Saber, R., “Near-identity diffeomorphisms and exponential/spl ϵ /tracking and/spl ϵ /stabilization of first-order nonholonomic SE (2) vehicles,” *American Control Conference, 2002. Proceedings of the 2002*, Vol. 6, IEEE, 2002, pp. 4690–4695.
- [40] Clancy, L. J., *Aerodynamics*, Halsted Press, 1975.
- [41] Stellato, B., Banjac, G., Goulart, P., Bemporad, A., and Boyd, S., “OSQP: An Operator Splitting Solver for Quadratic Programs,” *ArXiv e-prints*, 2017.
- [42] Blanchini, F., and Miani, S., *Set-theoretic methods in control*, Springer, 2008.